arXiv:1907.13349v1 [cs.CV] 31 Jul 2019

Competing Ratio Loss for Discriminative Multi-class Image Classification

Ke Zhang, Xinsheng Wang, Yurong Guo, Zhenbing Zhao, Zhanyu Ma, and, Tony X. Han

***Abstract*—The development of deep convolutional neural network architecture is critical to the improvement of image classification task performance. A lot of studies of image classification based on deep convolutional neural network focus on the network structure to improve the image classification performance. Contrary to these studies, we focus on the loss function. Cross-entropy Loss (CEL) is widely used for training a multi-class classification deep convolutional neural network. While CEL has been successfully implemented in image classification tasks, it only focuses on the posterior probability of correct class when the labels of training images are one-hot. It cannot be discriminated against the classes not belong to correct class (wrong classes) directly. In order to solve the problem of CEL, we propose Competing Ratio Loss (CRL), which calculates the posterior probability ratio between the correct class and competing wrong classes to better discriminate the correct class from competing wrong classes, increasing the difference between the negative log likelihood of the correct class and the negative log likelihood of competing wrong classes, widening the difference between the probability of the correct class and the probabilities of wrong classes. To demonstrate the effectiveness of our loss function, we perform some sets of experiments on different types of image classification datasets, including CIFAR, SVHN, CUB200-2011, Adience and ImageNet datasets. The experimental results show the effectiveness and robustness of our loss function on different deep convolutional neural network architectures and different image classification tasks, such as fine-grained image classification, hard face age estimation and large-scale image classification.**

***Index Terms*—Competing Ratio Loss, Cross-entropy Loss, Deep Convolutional Neural Networks, Image Classification**

I. Introduction

DEEP convolutional neural network (DCNN) has achieved great success in the most tasks of computer vision, such as image classification [1], [2], object detection [3], [4], image segmentation [5] and others, because DCNN can automatically learn optimal feature from inputs in an end-to-end manner. As the basis of computer vision technologies, image classification has been a research focus in artificial intelligence fields [6], [7]. In the image classification task, DCNNs learn to generate predicted distribution of image class by extracting depth features of input image [8]. The learning objective is to minimize the difference between the class distribution predicted by DCNNs and true data-generating distribution. To measure the difference, a multitude of loss functions are proposed, such as mean square error loss (MSE), hinge loss [9] and cross-entropy loss (CEL) [10]. These loss functions play important roles in the training of DCNNs. Compared with the other two loss functions, CEL has excellent convergence speeds for training DCNNs. Therefore, CEL is a reasonable loss function for classification tasks based on DCNNs.

CEL is popular for image classification task, however it also has disadvantages. The cross entropy between two probability

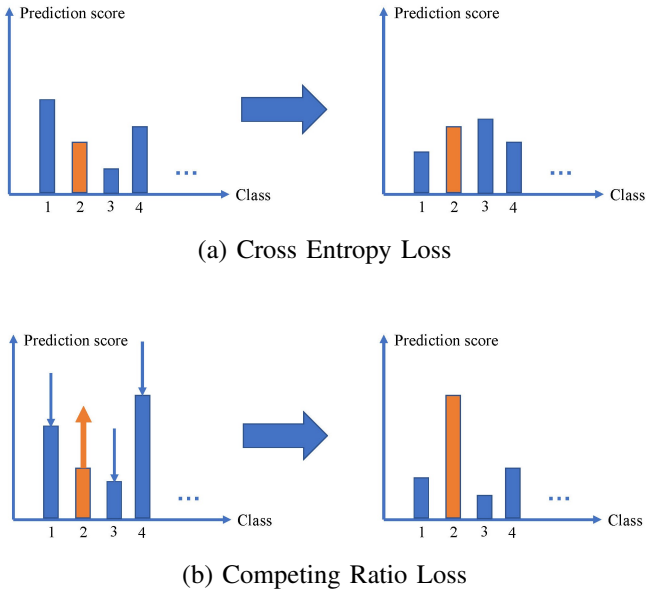

Fig. 1. Motivation of Competing Ratio Loss. (a) An explanation of cross entropy loss function, which focuses on the posterior probability of correct class when the labels of training images are one-hot. It cannot be discriminated against the classes not belong to correct class (wrong classes), when training classifier, the posterior probability of some wrong class will be probably increased. (b) The idea of competing ratio loss, which introduces competing ratio between the probability of the correct class and the probability of competing wrong classes, strengthen the posterior probability of correct class, and weaken the posterior probabilities of wrong classes, widening the difference between the probability of the correct class and the probabilities of wrong classes. The correct class can be discriminated against the competing wrong classes.

K. Zhang, X. Wang, Y. Guo and Z. Zhao are with Department of Electronic and Communication Engineering, North China Electric Power University, Hebei, China.
Z. Ma is with Beijing University of Posts and Telecommunications, Beijing, China.
T. X. Han is with Jingchi.ai, Guangzhou, China.
This work is supported in part by the National Natural Science Foundation of China (NSFC) under grant number 61871182,61302163, 61773071, 61401154, 61773160, by Beijing Natural Science Foundation under grant number 4192055, by the Natural Science Foundation of Hebei Province of China under grant number F2015502062, F2016502101, F2017502016, by the Fundamental Research Funds for the Central Universities under grant number 2018MS094, 2018MS095, and by the Open Project Program of the National Laboratory of Pattern Recognition (NLPR) under grant number 201900051.

distributions over the same set of events measures the average number of bits needed to identify an event drawn from the set if coding scheme obeyed a learned probability distribution, rather than the real but unknown distribution [10]. But in practice, i.e., when training DCNNs in the classification task, the real data-generating distribution is unknown and substituted by the empirical probability distribution over a training set. Each sample of the training set is independently and identically distributed (i.i.d) from the data space [11]. Under the assumption that both the image feature space and the label space obey uniform distribution, minimizing CEL is equivalent to maximizing likelihood. In other words, minimizing the CEL in training DCNNs is equivalent to maximizing the likelihood of training samples [8]. Maximum likelihood is a training criterion of machine learning, by which the network learns the likelihood of correct class for input sample. The network uses Bayes rules to calculate posterior probabilities of target classes for the input sample and then predicts the most likely class. We observed that when the labels of training samples are one-hot, this criterion cannot directly discriminate the posterior probability of correct class against the classes not belong to correct class (competing wrong classes), which only focuses on the posterior probability of correct class.

Inspired by this observation, we propose a discriminative competing ratio loss introducing the competing ratio between the posterior probability of the correct class and the posterior probabilities of competing wrong classes for input image to CEL, which aims to discriminate the posterior probability of correct class against the competing wrong classes, as shown in **Fig.1**. The contributions of our work are as follows:

1) We propose a new loss function for image classification, named competing ratio loss (CRL), to discriminate the posterior probability of correct class against the competing wrong classes. When training DCNNs, the posterior probability of correct class is increasing, the difference between the negative log likelihood of correct class and the negative log likelihood of competing wrong classes is increasing, the difference between the probability of the correct class and the probabilities of wrong classes is widening.

2) This loss function can be embedded into different types of DCNNs, such as ResNet [1], VGGNet [12] and be optimized via stochastic gradient descent (SGD) in an end-to-end manner.

3) The proposed loss is evaluated on a number of image classification datasets of different aspects (CIFAR-10/100 [13], SVHN [14], CUB200-2011 [15], Adience [16] and ImageNet [17]), and achieves better results than CEL, implying that CRL is effective and robust.

II. Related work

The performance improvement of image classification is inseparable from the development of the structure and depth of deep convolutional neural networks. Since AlexNet [18] won the ILSVRC2012 (Large Scale Visual Recognition Challenge 2012), which represented a significant advancement in image classification task, a lot of deep neural networks have been proposed. The VGGNet [12] improved the performance by deepening the depth of the network. GoogLeNets [19]–[23] enhanced the image feature extraction capabilities by using multiple scale convolution kernels on a single-layer convolutional layer. In order to reduce the difficulty of training deep convolutional neural networks, He et al. proposed ResNet [1], which introduced shortcut connections and residual representation into training deep networks. ResNet has a number of popular variants which explore the representation ability of DCNNs. Wide residual networks (WRNs) [24] widened the network by increasing the number of output channels in the convolutional layer. ResNeXt [25] increased the third dimensionalcardinality to improve image classification performance. Zhang et al. [26] proposed the multilevel residual network (RoR), which added level-wise shortcut connections upon original residual networks to promote the learning capability of residual networks. Then, they built pyramid multi-level residual network (P-RoR) [27] based on the pyramid residual network. To ensure maximum information flow between layers in the networks, Huang et al. [2] proposed DenseNet, of which each layer obtains additional inputs from all preceding layers and passes on its own feature maps to all subsequent layers. CondenseNet [28] was proposed to reduce memory of DenseNet by learning group convolution operations and pruning during training. In addition, the dual path network (DPN) [29] family combined ResNet which enabled feature reusage, and DenseNet which enabled new feature exploration. It achieved competitive results in image classification, object detection, and semantic segmentation tasks. Alternately updated clique (CliqueNet) [30] models incorporate both forward and backward connections between any two layers in the same block, which maximize information flow and achieve feature refinement. Zhang et al. proposed Multiple Feature Reweight DenseNet (MFR-DenseNet) [31] to improve the representation power of the DenseNet by adaptively recalibrating the channel-wise feature responses and explicitly modeling the interdependencies between the features of different convolutional layers.

However, after the network's depth, width and parameter quantities reach a certain level, even if the network's depth is further increased, the performance of classifier will not be greatly improved, but a large amount of computing resources will be consumed. Thus, some researchers turn their attention to other aspects of convolutional neural networks such as loss functions, optimizers. To train a classification network, cross entropy loss (CEL) is by far the most popular loss function for training networks. In addition, some existing works have attempted to improve original CEL from different aspects. Triplet Loss [32] focused on reducing the distance between the current sample and positive sample, and increased the distance for the negative ones. Center loss [33] was proposed to simultaneously learn a center for the deep features of each class and constrain the distances between the deep features and their corresponding class centers, which reduced intra-class variance. Liu et al. [34] proposed large-margin loss (L-Softmax) by adding angular constraints to each identity to encourage the discriminative learning of features by increasing inter-class separability and intra-class compactness. Large-margin loss have a lot of variant functions, such as Soft-Margin Softmax Loss [35], Angular Softmax (A-Softmax) [36] and so on. Soft-Margin Softmax Loss (SM-Softmax) used soft distant

margin to theoretically contain all the hard angle margin in L-Softmax and the degenerative margin in Softmax Loss. It not only inherited all merits from Softmax and L-Softmax but also learned features with large soft margin between different classes. A-Softmax [36] improved L-Softmax by normalizing the weights, which achieved better performance on a series of open-set face recognition benchmarks. Li et al. [4] proposed focal loss (FL) to address this class imbalance by reshaping the standard CEL such that it down-weighted the loss assigned to well-classified examples. Li et al. [37] added a regularization term to cross entropy loss, which can place a constraint on the probability that a data point is assigned to a class other than its ground-truth class. Martinez et al. [38] proposed taming cross entropy loss (TCE) which is more robust to noise and outliers.

III. Competing Ratio Loss Function

An image classification task is to categorize an image to one of the target classes. Suppose $\mathbf{x}$ is the feature vector representing the image, y is the class that the image belongs to. Then the goal of the image classification task is to find a function $y = f(\mathbf{x}, y)$ that can predict y from $\mathbf{x}$. However, there exists misclassification risk due to a series of factors such as noise, missing information. Thus the learning goal of the image classification task is to minimize the risk, defined as

$$R(f) = \mathbf{E}_{X,Y\sim(\mathbf{x},y)} L(f(\mathbf{x}), y) \tag{1}$$

where $L(f(\mathbf{x}), y)$ is a loss function measuring the cost of misclassification. $p(\mathbf{x}, y)$ is the probability density function over the image feature space X and the class label space Y. Because $p(\mathbf{x}, y)$ is real but unknown data-generating probability distribution, we generate a training set in which the samples are independently and identically distributed (i.i.d.)

$$S_m = \{(x_1, y_1), \cdots, (x_i, y_i), \cdots, (x_m, y_m)\} \tag{2}$$

The training set S consists of m samples, where (x_i, y_i) is the ith ($i \in \{1, 2, \cdots, m\}$) sample. y_i is the label of x_i. Then the risk of misclassification can be approximated as

$$R_S(f) = \frac{1}{m} \sum_{i=1}^{m} L(f(x_i), y_i) \tag{3}$$

The loss function L is differently defined in different tasks.

A. Cross Entropy Loss Function

Cross entropy loss (CEL) is the most popular loss function for training a multi-class classifier based on deep convolutional neural network (DCNN), because it measures the difference between the target class distribution and the predicted class distribution, and can be reduced by stochastic gradient descent (SGD). Suppose all images have C target classes in the image classification task. The DCNN takes the image x_i as input and outputs C nodes. Each node represents the score of corresponding class. When the activation function in the output layer is defined as a softmax function, the C outputs can be regarded as the posterior probabilities of classes [39]: $\hat{p}(y_c|x)$, $c = 1, 2, \cdots, C$, where x is the input vector of DCNN. Therefore, CEL is defined as

$$L_{CEL} = -\sum_{c=1}^{C} p(y_c|x) \log \hat{p}\,(y_c|x) \tag{4}$$

where $p(y_c|x)$ is the empirical distribution of the training set, and $\hat{p}(y_c|x)$ is the predicted distribution from the DCNN model. In the specific (and usual) case of multi-class image classification the images' labels are one-hot. In other words, each training image is labeled as the correct class it belongs to

$$p(y_c|x) = \begin{cases} 1 & \text{if } x \in y_c \\ 0 & \text{otherwise} \end{cases} \tag{5}$$

Under the condition of Equation (5), Equation (4) can be rewritten as

$$L_{CEL} = -\log \hat{p}(y_c|x) \tag{6}$$

Equation (6) shows that when the labels of training images are one-hot, CEL only focuses on the probability that an image is assigned to its ground-truth class and does not place any focus on the probability that the image is assigned to a class other than its ground-truth class (competing wrong class), as shown in **Fig.1(a)**. **Fig.1(a)** shows that the probability distribution change of the prediction when minimizing CEL. The figure shows the probabilities of some classes increase, and the probabilities of some classes decrease, except for the probability of correct class. CEL cannot directly discriminate the posterior probability of correct class against the competing wrong classes.

In binary classification task where there are two target classes, a DCNN can be designed with one single output for which the empirical probability $p(y_c|x)$ equals 1 for one class and 0 for the other class. Then Equation (4) can be simplified to a binary cross-entropy loss function (BCE) [39] as

$$\begin{aligned} L_{BCE} = &-p(y_c|x) \log \hat{p}(y_c|x) \\ &-[1 - p(y_c|x)] \log [1 - \hat{p}(y_c|x)] \end{aligned} \tag{7}$$

According to Equation (5), the binary cross-entropy loss function can be extended to the multi-class classification task as

$$\begin{aligned} L_{MCE} &= -\log \hat{p}(y_c|x) - \sum_{k=1, k\neq c}^{C} \log[1 - \hat{p}(y_k|x)] \\ &= -\log[\hat{p}(y_c|x) \prod\nolimits_{k=1,k\neq c}^{C} \hat{p}(\bar{y_k}|x)] \end{aligned} \tag{8}$$

where $\hat{p}(\bar{y_k}|x) = 1 - \hat{p}(y_k|x)$ represents the probability of x not classified as y_k. In other words, $\hat{p}(\bar{y_k}|x)$ is the predicted probability of x belongs to the competing wrong classes. Comparing Equation (6) and Equation (8), we can know that each $\hat{p}(y_c|x)$ is multiplied by a factor $\prod_{k=1,k\neq c}^{C} \hat{p}(\bar{y_k}|x)$ which is product of probabilities of belonging to each of competing wrong classes. Although Equation (8) consists of probabilities of competing wrong classes, it does not also discriminate the correct class probability from the competing wrong ones.

In addition, as we know, CEL can be backpropagated when training DCNNs. Supposed that a softmax layer is connected with DCNN. We denote $\hat{p}(y_c|x)$ as p_c, $\hat{p}(y_k|x)$ as p_k. p_c and

p_k are outputs of the softmax layer. The softmax function guarantees $p_c + \sum_{k=1,k\neq c}^{C} p_k = 1, p_c \in (0,1)$. Therefore Equation (6) can be written as

$$L_{CEL} = -\log p_c \tag{9}$$

The softmax layer outputs p_c. The derivative of p_c with respect to x_j in softmax function is

$$\frac{\partial p_c}{\partial x_j} = \begin{cases} p_c(1-p_j) & c \neq j \\ -p_c p_j & c = j \end{cases} \tag{10}$$

Therefore the derivative of CEL with respect to x_j is

$$\begin{aligned} \frac{\partial L_{CEL}}{\partial x_j} = \frac{\partial L_{CR}}{\partial p_c} \times \frac{\partial p_c}{\partial x_j} = \\ (-\frac{1}{p_c}) \times (-p_c p_j) = p_j \end{aligned} \tag{11}$$

From Equation (11), we can know that, the gradient that CEL updates when backpropagating is not relevant to p_c.

B. Competing Ratio Loss Function

In this section, we propose a new loss function that discriminates the correct class and the competing wrong classes when the labels of training images are one-hot. As discussed in section **III-A**, minimizing CEL is equivalent to maximizing likelihood. However, CEL only measures the probability of the correct class for each input image. It cannot learn to discriminate between the correct class probability and the competing wrong classes probabilities. To overcome the shortcoming of CEL, under the condition of Equation (5), we propose to calculate the ratio between the predicted correct-class probability and the probabilities of competing wrong classes in competing ratio loss function (CRL) for the image classification task, to widen the difference between the probability of the correct class and the probabilities of competing wrong classes. The CRL is defined as

$$L_{CRL} = \log \frac{\sum_{k=1,k\neq c}^{C} \hat{p}(y_k|x)}{\hat{p}(y_c|x)} \tag{12}$$

Equation (12) shows that when the posterior probability of the correct class increasing, the ratio between the correct class probability and the competing wrong classes probabilities is decreasing. The difference between the correct class probability and the competing wrong classes probabilities is widen.

In addition, the numerator on the right side of Equation (12) is sum of competing class probabilities representing the probability of not belonging to the correct class, denoted as $\hat{p}(\bar{y_c}|x)$. Since the image feature distribution $p(x)$ and the class label distribution $p(y)$ are not relevant to the CNN parameters and obeying uniform distributions, according the Bayesian inference, Equation (6) can be rewritten as

$$L_{CEL} = -\log \hat{p}(x|y_c) \tag{13}$$

Equation (12) can be rewritten as

$$\begin{aligned} L_{CRL} &= \log \hat{p}(\bar{y_c}|x) - \log \hat{p}(y_c|x) \\ &= \log \hat{p}(x|\bar{y_c}) - \log \hat{p}(x|y_c) \\ &= -[\log \hat{p}(x|y_c) - \log \hat{p}(x|\bar{y_c})] \end{aligned} \tag{14}$$

Equation (13) shows that CEL is negative log likelihood of the image x. Equation (14) shows that CRL is the difference between the negative log likelihood of correct class and the negative log likelihood of competing wrong classes. It directly discriminates the correct class from the competing wrong classes for each training image when training DCNN.

We denote $\hat{p}(y_k|x)$ as p_k, $\hat{p}(y_c|x)$ as y_c. p_k and p_c are the outputs of softmax layer. The softmax function guarantees $p_c + \sum_{k=1,k\neq c}^{C} p_k = 1, p_c \in (0,1)$. Therefore Equation (12) can be written as

$$\begin{aligned} L_{CRL} &= \log \frac{1-p_c}{p_c} \\ &= \log(1-p_c) - \log p_c \\ &= \log(1-p_c) + L_{CEL} \end{aligned} \tag{15}$$

Obviously, when $p_c \in (0, 0.5)$, $\log \frac{(1-p_c)}{p_c} > 0$. When $p_c \in (0.5, 1)$, $\log \frac{(1-p_c)}{p_c} < 0$. Equation (15) shows that CRL can be regard as a combination of CEL and a regularization term. The regularization term is responsible for changing the ratio between the predicted correct-class probability and the probability of competing wrong classes. To guarantee the value of CRL is greater than 0, we add the hyper-parameter α to $1 - p_c$. In addition, we use the hyper-parameter β control the weight of competing ratio. Therefore, CRL with hyper-parameters α and β is defined as

$$\begin{aligned} L_{CRL} &= \log \frac{(\alpha + \sum_{k=1,k\neq c}^{C} \hat{p}(y_k|x))^{\beta}}{\hat{p}(y_c|x)} \\ &= \beta \log(\alpha + \sum_{k=1,k\neq c}^{C} \hat{p}(y_k|x)) \\ &\quad - \log \hat{p}(y_c|x) \\ &= \beta \log(\alpha + \sum_{k=1,k\neq c}^{C} \hat{p}(y_k|x)) \\ &\quad + L_{CEL} \\ &= \beta \log(\alpha + 1 - p_c) + L_{CEL} \end{aligned} \tag{16}$$

Equation (12) and (16) show that it directly learns to discriminate correct class from the competing wrong classes for each training image, as shown in **Fig.1(b)**. In addition, when $\beta = 0$, CRL is equivalent to CEL.

C. Derivative of the Competing Ratio Loss Function

We denote $\hat{p}(y_c|x)$ as y_c. The softmax layer outputs p_c. the derivative of CRL with respect to x_j is

$$\begin{aligned} \frac{\partial L_{CRL}}{\partial x_j} = \frac{\partial L_{CRL}}{\partial p_c} \times \frac{\partial p_c}{\partial x_j} = \\ (\frac{\beta}{\alpha + 1 - p_c} - \frac{1}{p_c}) \times (-p_c p_j) = \\ (1 - \frac{\beta p_c}{\alpha + 1 - p_c}) p_j \end{aligned} \tag{17}$$

Equation (17) shows the derivative of CRL can be propagated using the standard back propagation method. Compared

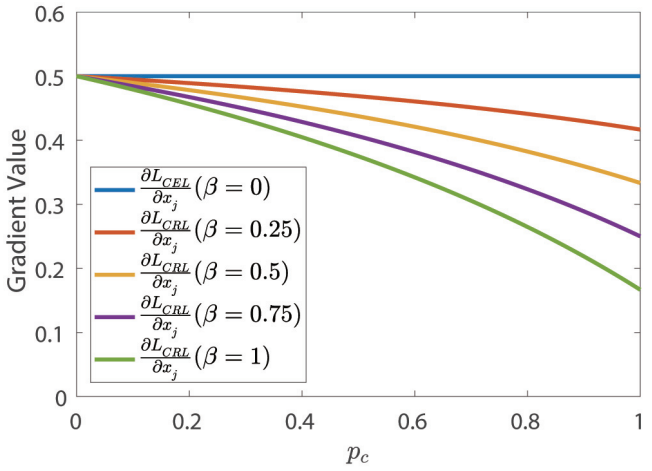

Fig. 2. The trend of CRL and CEL's gradient value against x_j with p_c. The blue line shows the trend of CEL gradient value against x_j with p_c. The others line show the trend of CRL gradient value against x_j with p_c when β takes different values.

Equation (17) and Equation (11), we can observe that the differentiation of CRL is relevant to p_c. **Fig.2** shows the trend of CRL and CEL's gradient value against x_j with p_c. For the convenience of drawing the figure, we make $\alpha = 1.5$, $p_j = 0.5$ in Equation (11) and (17). When p_c increases, the gradient value of CRL relative to x_j is decreasing. However, the gradient value of CEL relative to x_j is constant with respect to x_j. Thus, CRL's update step size in SGD is dependent of the confidence estimate of the correct class in the classification prediction. When p_c increases, the update step size is decreasing. It illustrates that when CNN classifier has higher probability of the correct class, the parameter amount of CNN updated by backpropagation becomes smaller, maintaining high confidence in the correct class of images by CNN classifier. On the contrary, when p_c decreases, the update step size is increasing. CNN classifier has higher probabilities of the wrong classes, the parameter amount of CNN updated by backpropagation becomes larger, making CNN tend to increase the probability of the correct class. It indicates that the CRL is adaptive to the probability of correct class in backpropagation. When the probability of correct class is high, CNN updates a small number of parameters. When the probability of correct class is low, CNN updates a large number of parameters to increase the probability of correct class. Compared with CRL, the update size of backpropagation using CEL is constant whatever the probability of the correct class is high or low. CEL is unchanged for the probability of the correct class. Moreover, the hyper-parameter β can influence the update step size of the CRL, as shown in **Fig.2**. From Equation (17), we can obviously draw such a conclusion that when β increases, the gradient value of CRL relative to x_j is decreasing, maintaining higher confidence in the correct classification of images during backpropagation.

IV. Experiments and Results

In this section, we show implementation details and experimental results. First, we show how two hyper-parameters α and β influence the CRL. Then we show the robustness and effectiveness of CRL in different-depth DCNNs and different types of DCNNs. Finally, we show our CRL outperforms CEL on several popular image classification datasets.

A. Experiments Setup

1) Datasets: **CIFAR10/100** [13] consist of colored natural scene images, with 32×32 pixels each. The training set and test set contain 50,000 and 10,000 images respectively. CIFAR-10 images are drawn from 10 classes, and the CIFAR-100 images are drawn from 100 classes. We adopt a standard data augmentation scheme in our experiments: random sampling and horizontal flipping.

The Street View House Numbers (**SVHN**) [14] dataset contains 32×32 colored digit images. There are 73,257 images in the training set, 26,032 images in the test set, and 531,131 images for additional training. For training network, we use all the training data without any data augmentation.

Adience [16] dataset is proposed for facilitating the study of age estimation in the wild, which is difficult to classify due to the similarity between adjacent age groups. The entire Adience collection includes 26,580 256×256 color facial images of 2,284 subjects, with eight classes of age groups (0-2, 4-6, 8-13, 15-20, 25-32, 38-43, 48-53, 60-100). In this article, testing for age group classification is performed using a standard five-fold, subject-exclusive cross-validation protocol, defined in [16].

CaltechUCSD Birds (**CUB-200-2011**) [15] is a challenging dataset, which aims to distinguish subordinate-level bird species, with photos of 200 bird species, each species with roughly 30 training images and 30 testing images, and has become a staple for testing new ideas for fine-grained image classification.

The ILSVRC 2012 classification dataset (**ImageNet**) [17] is the largest large-scale image classification dataset currently, consisting of 1.2 million images for training, and 50,000 for validation, from 1,000 classes. We adopt the same data augmentation scheme for training images as in [2], and apply a single-crop with size 224×224 at test time.

2) Network used and training strategies: For comparison, the experiments in this paper use ResNet [1] and VGG [12] networks. On CIFAR datasets, the networks are trained using stochastic gradient descent (SGD) for 300 epochs with a mini-batch size of 256. We use a weight decay of 1e-4, Nesterov momentum of 0.9. The learning rate starts from 0.1, and is divided by 10 at 50% and 75% of the training procedure. On SVHN and CUB200-2011 datasets, the network are trained using SGD for 40 epochs with a mini-batch size of 64. The learning rate start from 0.1, and are divided by 10 at 50% and 75% of the training procedure. On Adience dataset, the total epoch number is 120. The learning rate starts from 0.1, and is divided by the factor of 10 and 100 after epoch 60 and 80. On ImageNet, we train models for 90 epochs with a batch size of 256. The learning rate is set to 0.1 initially, and is lowered by 10 times at epoch 30 and 60. All experiments are implemented on Pytorch 0.4 with one NVIDIA GeForce GTX TITAN X Pascal GPU.

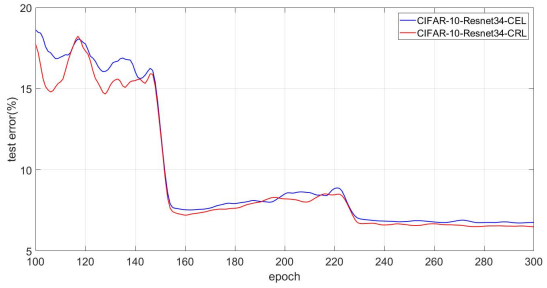

(a) Smoothed test errors on CIFAR-10 by ResNet34

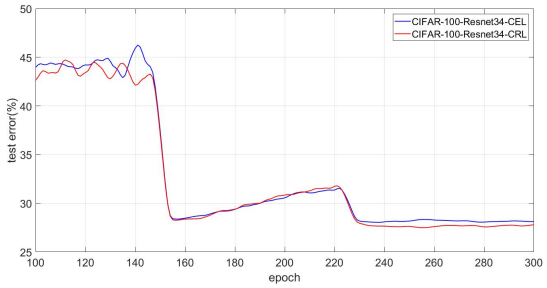

(b) Smoothed test errors on CIFAR-100 by ResNet34

Fig. 3. Smoothed test errors on CIFAR-10/100 by ResNet34

TABLE I
TEST ERRORS (%) ON CIFAR-10/100 UNDER DIFFERENT HYPER-PARAMETERS α AND β BY RESNET34

CIFAR-10	α**=1**	α**=1.5**	α**=2**
β**=0**		6.63	
β**=0.25**	6.48	6.33	6.44
β**=0.5**	6.18	6.08	6.23
β**=0.75**	6.28	6.07	6.18
β**=1**	6.41	**5.99**	6.1
CIFAR-100	α**=1**	α**=1.5**	α**=2**
β**=0**		27.87	
β**=0.25**	28.14	27.39	26.78
β**=0.5**	27.56	27.93	27.18
β**=0.75**	27.53	27.36	27.47
β**=1**	27.34	**27.26**	27.54

B. Influences of the parameters α and β

There are two hyper-parameters α and β. Since in Equation (16), α guarantees the loss function is greater than 0, β is the weight of competing ratio, we evaluate their influences in image classification on CIFAR-10 and CIFAR-100 using the ResNet34 [1] model. We set α three values: 1.0, 1.5 and 2.0. We set β five values: 0, 0.25, 0.5, 0.75 and 1. **Table I** shows the influence of hyper-parameters α and β. We can see that when α is fixed to a constant, β changes from 0 to 1, test errors have a tendency to decline. When β is equal to 1, the test error rate is the lowest value. It indicates that when β increases, CNN maintains higher confidence in the correct classification of images during backpropagation. In addition, when β is fixed to a constant, test errors of $\alpha = 1.5$ are lower than others. Therefore, according to the ablation experiments in this section, in the following experiments, we set $\alpha = 1.5$, $\beta = 1$, which are the most efficient hyper-parameters.

TABLE II
TEST ERRORS (%) ON CIFAR-10/100 BY DIFFERENT-DEPTH AND DIFFERENT KINDS OF NETWORKS

CIFAR-10	**CEL**	**CRL**(α**=1.5**, β**=1**)
VGG16 [12]	6.32	6.27
VGG19 [12]	6.28	6.06
ResNet34 [1]	6.63	5.99
ResNet50 [1]	5.9	5.6
ResNet101 [1]	5.49	5.37
ResNet164 [1]	4.76	**4.36**
CIFAR-100	**CEL**	**CRL**(α**=1.5**, β**=1**)
VGG16 [12]	26.97	26.63
VGG19 [12]	26.8	26.24
ResNet34 [1]	27.87	27.34
ResNet50 [1]	25.33	25.23
ResNet101 [1]	24.27	23.34
ResNet164 [1]	22.26	**21.94**

TABLE III
TEST ERRORS (%) ON CIFAR-10/100 USING DIFFERENT LOSS FUNCTIONS BY RESNET164

	CEL [1]	**FL** [4]	**TCE** [38]	**CRL**
CIFAR-10	5.27	4.62	5.46	**4.36**
CIFAR-100	22.26	22.13	23.93	**21.94**

C. Experiments on different networks and different-depth networks

In this section, we evaluate CRL on different networks and different-depth networks including ResNet34/50/101/164 [1], VGG16/19 [12]. **Table II** shows the test errors on CIFAR-10 and CIFAR-100. **Fig.3** shows smoothed test errors on CIFAR-10/100 by ResNet34, corresponding to results in **Table II**. We can see that CRL outperforms CEL on different-depth and different kinds of models. These results demonstrate the effectiveness and robustness of CRL. No matter what kinds of DCNN are available, CRL can always achieve better results than its basic DCNN with the same number of layers. Besides, from **Fig.3**, we can see that on CIFAR-10/100, CRL has faster gradient convergence than CEL from epoch 100-150, when learning rate is 0.1, because CRL is adaptive to the probability of correct class in backpropagation, as analyzed in section III-C.

D. Compared with the other loss functions under the same conditions

Table III compares CRL and other popular loss functions by ResNet164 model on CIFAR-10/100 datasets, including cross-entropy loss (CEL), focal loss (FL) [4] and taming cross-entropy loss (TCE) [38]. We don't directly use the results in the paper, but re-run these loss functions on ResNet164 model. Our CRL outperforms the other loss functions obviously suggesting that CRL is effective. Through experiments, we argue that our CRL can improve the discrimination ability by computing the competing ratio between correct class and competing wrong classes.

E. Generalization on some image classification datasets

In order to experimentalize the generalization of our proposed CRL in different image classification tasks, we experiment our proposed CRL and CEL by ResNet34 [1] on

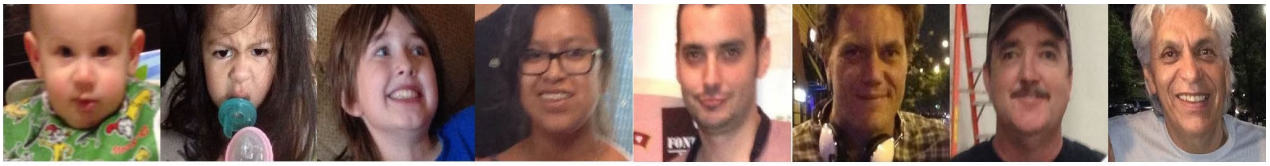

Figure	A1	B1	C1	D1	E1	F1	G1	H1
Labeled Class	0-2	4-6	8-13	15-20	25-32	38-43	48-53	60-100
CRL	0-2	4-6	8-13	15-20	25-32	38-43	48-53	60-100
CEL	0-2	4-6	8-13	15-20	25-32	38-43	48-53	60-100

(a) Good results of using our CRL and CEL.

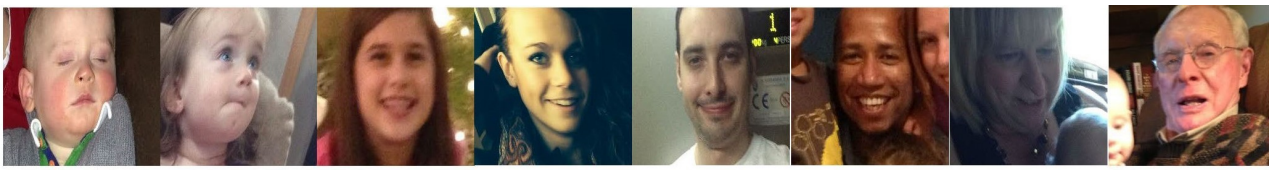

Figure	A2	B2	C2	D2	E2	F2	G2	H2
Labeled Class	0-2	4-6	8-13	15-20	25-32	38-43	48-53	60-100
CRL	0-2	4-6	8-13	15-20	25-32	38-43	48-53	60-100
CEL	4-6	8-13	25-32	48-53	48-53	25-32	60-100	48-53

(b) Good results using our CRL and bad results using CEL

Fig. 4. Examples of age group classification results by ResNet34 using CEL and CRL. The top row shows good results of using our CRL and CEL. The below row shows good results using our CRL but bad results using CEL. The table below each image shows the labeled class and the classification results using our CRL and CEL.

TABLE IV
CLASSIFICATION ERROR RATE OR ACCURACY RATES (%) ON SEVERAL IMAGE CLASSIFICATION DATASETS USING CRL AND CEL BY RESNET34 [1]. IN THE SVHN AND IMAGENET LINE, WE USE CLASSIFICATION ERROR RATE. IN THE OTHERS LINE, WE USE CLASSIFICATION ACCURACY. IN THE ADIENCE LINE, THE CONTENT OUTSIDE THE BRACKETS REPRESENTS THE EXACT CLASSIFICATION ACCURACY, THE CONTENT IN BRACKETS REPRESENTS WITH-ONE-CATEGORY-OFF ACCURACY [40]. IN THE IMAGENET LINE, THE CONTENT OUTSIDE THE BRACKETS REPRESENTS TOP-1 ERROR, THE CONTENT IN PARENTHESES REPRESENTS TOP-5 ERROR [17].

	CEL	CRL
SVHN	3.82	3.43
CUB200-2011	53.09	55.26
Adience	56.32(90.99)	57.05(91.26)
ImageNet	27.09(8.95)	26.94(8.69)

several datasets of different aspects, including Adience [16], SVHN [14], CUB200-2011 [15] and ImageNet ILSVRC 2012 dataset [17], which are popular image classification datasets. The results of test sets are reported in **Table IV**. It can be seen that on the SVHN dataset, the classification error rate of CRL is 3.43%, which is about 10.2% lower than CRL. Then experimental result shows that the proposed loss achieves competitive performance on the SVHN dataset.

On the CUB200-2011 dataset, our proposed CRL improves 4.087% upon the performance of CEL in fine-grained image classification. CUB-200-2011 is a challenging dataset, which aims to distinguish subordinate-level bird species. Our proposed CRL improves the ability to distinguish fine-grained categories by maximizing the ratio between the correct class probability and competing wrong classes.

The Adience dataset is difficult to classify due to the similarity between adjacent age groups. **Table IV** shows the exact classification accuracy and with-one-category-off accuracy using CRL and CEL. Our CRL increases 0.73% on exact accuracy absolutely, 0.27% on with-one-category-off accuracy than CEL absolutely. **Fig.4** shows examples of age group classification results by ResNet34 using CEL and CRL on the Adience dataset. The top row shows good results of using our CRL and CEL. The below row shows good results using our CRL but bad results using CEL. We can observe that the proposed loss is more robust to most of the common facial appearance variations than CEL, such as multi-face in the image (F2, G2), illumination (D2), filming angle (H2) and so on. **Fig.5** shows the softmax output heatmap of example images corresponding to **Fig.4**. We can see that our proposed loss makes the softmax output on the diagonal line of heatmap, which shows CRL makes the prediction probability of the correct class as high as possible, weakens the prediction probabilities of the competing wrong classes. For example, observing the softmax output of the image G1 using CRL and CEL, we can get a conclusion that when the prediction probabilities of some adjacent classes including the correct class, our CRL can make the prediction probability of the correct class higher than other adjacent classes to the correct class. Observing the softmax output of the image C2 using CRL and CEL, our CRL can concentrate on the correct class

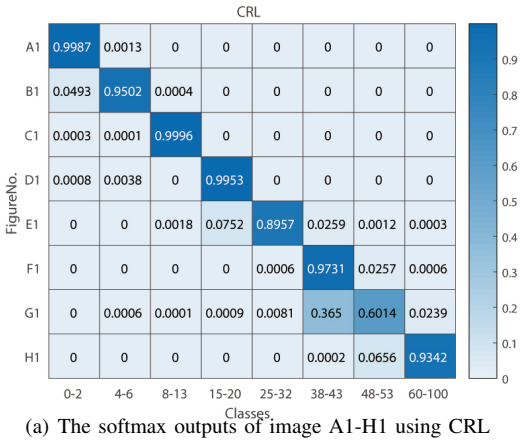

(a) The softmax outputs of image A1-H1 using CRL

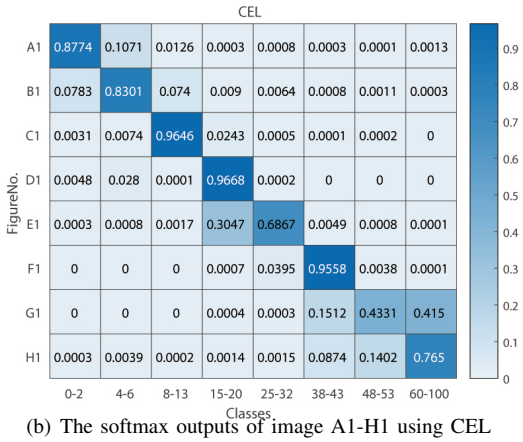

(b) The softmax outputs of image A1-H1 using CEL

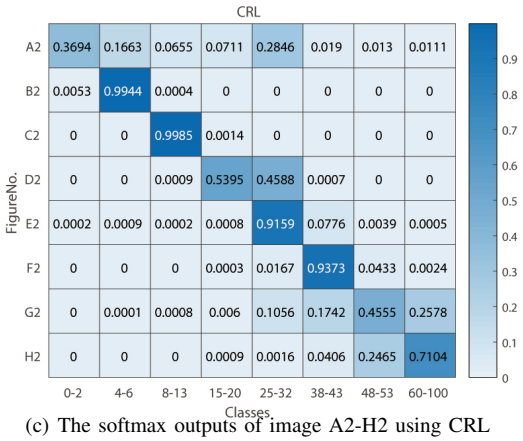

(c) The softmax outputs of image A2-H2 using CRL

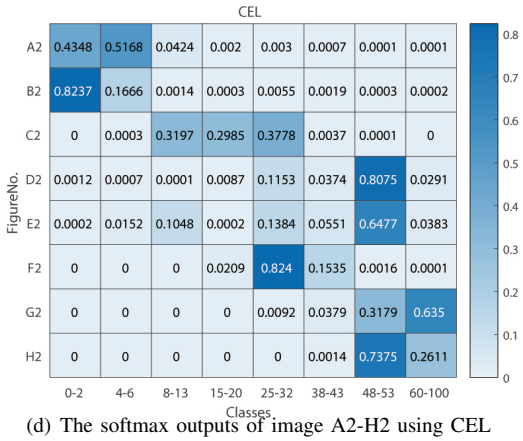

(d) The softmax outputs of image A2-H2 using CEL

Fig. 5. The softmax output heatmap of example images corresponding to **Fig.4**. The horizontal axis of each heatmap represents the prediction class. The vertical axis represents the example image's number. Each number in each heatmap is the probability of each class. Subfigure (a) and (b) are the softmax outputs of good results of using our CRL and CEL. Subfigure (c) and (d) are the softmax outputs of good results of using our CRL but bad results of using CEL.

however CEL classifies wrongly. The results demonstrated the consistent improvements of our CRL over the CEL in the hard face age estimation tasks.

In addition, **Table IV** also shows the Top-1 and Top-5 error of using CRL and CEL on the ImageNet, which is currently the largest large-scale image classification dataset. Compared with CEL, our CRL outperforms 0.15% on Top-1 error absolutely, 0.26% on Top-5 error absolutely. Because the amount of ImageNet is large enough, both CRL and CEL can fit the ImageNet well, although the improvement of CRL is not high, it verifies the effectiveness of CRL on large-scale image datasets.

V. Conclusion

In this paper we proposed a loss function competing ratio loss function (CRL) which discriminates the correct class probability from the competing wrong ones. The proposed loss calculates the ratio between the correct class probability and competing wrong classes. This ratio strengthens the posterior probability of correct class, and weakens the posterior probabilities of wrong classes. The results of a series of experiments show that compared with CEL, our proposed loss (1) can improve the discrimination ability by computing the competing ratio between correct class and competing wrong classes, which is the difference between the negative log likelihood of the correct class and the negative log likelihood of competing classes; (2) has better performance on different image classification tasks include fine-grained classification, hard face age estimation task and large-scale image classification.

Acknowledgment

The authors gratefully acknowledge the support of NVIDIA Corporation with the donation of the GPU used for research.

References

[1] K. He, X. Zhang, S. Ren, and J. Sun, "Deep residual learning for image recognition," in *Proceedings of the IEEE conference on computer vision and pattern recognition*, vol. 7, 2016, pp. 770–778.

[2] G. Huang, Z. Liu, L. Van Der Maaten, and K. Weinberger, "Densely connected convolutional networks," in *2017 IEEE Conference on Computer Vision and Pattern Recognition*, 2017, pp. 2261–2269.

[3] S. Ren, K. He, R. Girshick, and J. Sun, "Faster r-cnn: Towards real-time object detection with region proposal networks," in *Advances in neural information processing systems*, 2015, pp. 91–99.

[4] T.-Y. Lin, P. Goyal, R. Girshick, K. He, and P. Dollár, "Focal loss for dense object detection," in *Proceedings of the IEEE international conference on computer vision*, 2017, pp. 2980–2988.

[5] V. Badrinarayanan, A. Kendall, and R. Cipolla, "Segnet: A deep convolutional encoder-decoder architecture for image segmentation," *IEEE transactions on pattern analysis and machine intelligence*, vol. 39, no. 12, pp. 2481–2495, 2017.

[6] Y. Lecun, Y. Bengio, and G. Hinton, "Deep learning." *Nature*, vol. 521, p. 436, 2015.

[7] J. Gu, Z. Wang, J. Kuen, and et al., "Recent advances in convolutional neural networks," *Pattern Recognition*, vol. 77, pp. 354–377, 2018.

[8] I. Goodfellow, Y. Bengio, and A. Courville, *Deep Learning*. MIT Press, 2016.

[9] K. Duan and S. Keerthi, "Which is the best multiclass svm method? an empirical study," in *International workshop on multiple classifier systems*, 2005, pp. 278–285.

[10] D. B. Pieter Tjerk, D. P. Kroese, S. Mannor, and R. Rubinstein, "A tutorial on the cross-entropy method," *Annals of Operations Research*, vol. 134, no. 1, pp. 19–67, Feb 2005.

[11] V. Vapnik, *The nature of statistical learning theory*. Springer science, 2013.

[12] K. Simonyan and A. Zisserman, "Very deep convolutional networks for large-scale image recognition," *arXiv preprint arXiv:1409.1556*, 2014.

[13] A. Krizhevsky and G. Hinton, "Learning multiple layers of features from tiny images," Citeseer, Tech. Rep., 2009.

[14] Y. Netzer, T. Wang, A. Coates, A. Bissacco, B. Wu, and A. Y. Ng, "Reading digits in natural images with unsupervised feature learning," in *NIPS Workshop on Deep Learning and Unsupervised Feature Learning 2011*, 2011.

[15] C. Wah, S. Branson, P. Welinder, P. Perona, and S. Belongie, "The Caltech-UCSD Birds-200-2011 Dataset," California Institute of Technology, Tech. Rep., 2011.

[16] E. Eidinger, R. Enbar, and T. Hassner, "Age and gender estimation of unfiltered faces," *IEEE Transactions on Information Forensics and Security*, vol. 9, no. 12, pp. 2170–2179, 2014.

[17] O. Russakovsky, J. Deng, H. Su, J. Krause, S. Satheesh, S. Ma, Z. Huang, A. Karpathy, A. Khosla, M. Bernstein, A. C. Berg, and L. Fei-Fei, "ImageNet Large Scale Visual Recognition Challenge," *International Journal of Computer Vision*, vol. 115, no. 3, pp. 211–252, 2015.

[18] A. Krizhevsky, I. Sutskever, and G. E. Hinton, "Imagenet classification with deep convolutional neural networks," in *Advances in neural information processing systems*, 2012, pp. 1097–1105.

[19] C. Szegedy, W. Liu, Y. Jia, P. Sermanet, S. Reed, D. Anguelov, D. Erhan, V. Vanhoucke, and A. Rabinovich, "Going deeper with convolutions," in *Proceedings of the IEEE conference on computer vision and pattern recognition*, 2015, pp. 1–9.

[20] S. I. andChristian Szegedy, "Batch normalization: Accelerating deep network training by reducing internal covariate shift," in *International Conference on Machine Learning*, 2015, pp. 448–456.

[21] C. Szegedy, V. Vanhoucke, S. Ioffe, J. Shlens, and Z. Wojna, "Rethinking the inception architecture for computer vision," in *Proceedings of the IEEE conference on computer vision and pattern recognition*, 2016, pp. 2818–2826.

[22] C. Szegedy, S. Ioffe, V. Vanhoucke, and A. A. Alemi, "Inception-v4, inception-resnet and the impact of residual connections on learning," in *Thirty-First AAAI Conference on Artificial Intelligence*, 2017.

[23] F. Chollet, "Xception: Deep learning with depthwise separable convolutions," in *Proceedings of the IEEE conference on computer vision and pattern recognition*, 2017, pp. 1251–1258.

[24] S. Zagoruyko and N. Komodakis, "Wide residual networks," in *BMVC*, 2016, pp. 87.1–87.12.

[25] S. Xie, R. Girshick, P. Dollár, Z. Tu, and K. He, "Aggregated residual transformations for deep neural networks," in *Proceedings of the IEEE conference on computer vision and pattern recognition*, 2017, pp. 1492–1500.

[26] K. Zhang, M. Sun, T. X. Han, X. Yuan, L. Guo, and T. Liu, "Residual networks of residual networks: Multilevel residual networks," *IEEE Transactions on Circuits and Systems for Video Technology*, vol. 28, no. 6, pp. 1303–1314, 2018.

[27] K. Zhang, L. Guo, C. Gao, and Z. Zhao, "Pyramidal ror for image classification," *Cluster Computing*, no. 7553, pp. 1–11, 2017.

[28] G. Huang, S. Liu, L. Van der Maaten, and K. Q. Weinberger, "Condensenet: An efficient densenet using learned group convolutions," in *Proceedings of the IEEE Conference on Computer Vision and Pattern Recognition*, 2018, pp. 2752–2761.

[29] Y. Chen, J. Li, H. Xiao, X. Jin, S. Yan, and J. Feng, "Dual path networks," in *Advances in Neural Information Processing Systems*, 2017, pp. 4467–4475.

[30] Y. Yang, Z. Zhong, T. Shen, and Z. Lin, "Convolutional neural networks with alternately updated clique," in *Proceedings of the IEEE Conference on Computer Vision and Pattern Recognition*, 2018, pp. 2413–2422.

[31] K. Zhang, Y. Guo, X. Wang, J. Yuan, and Q. Ding, "Multiple feature reweight densenet for image classification," *IEEE Access*, vol. 7, pp. 9872–9880, 2019.

[32] F. Schroff, D. Kalenichenko, and J. Philbin, "Facenet: A unified embedding for face recognition and clustering," in *2015 IEEE Conference on Computer Vision and Pattern Recognition*, June 2015, pp. 815–823.

[33] Y. Wen, K. Zhang, Z. Li, and Y. Qiao, "A discriminative feature learning approach for deep face recognition," in *European Conference on Computer Vision*, 2016, pp. 499–515.

[34] W. Liu, Y. Wen, Z. Yu, and M. Yang, "Large-margin softmax loss for convolutional neural networks." in *International Conference on Machine Learning*, 2016, pp. 507–516.

[35] X. Liang, X. Wang, Z. Lei, S. Liao, and S. Z. Li, "Soft-margin softmax for deep classification," in *International Conference on Neural Information Processing*, 2017, pp. 413–421.

[36] W. Liu, Y. Wen, Z. Yu, M. Li, B. Raj, and L. Song, "Sphereface: Deep hypersphere embedding for face recognition," in *Proceedings of the IEEE conference on computer vision and pattern recognition*, 2017, pp. 212–220.

[37] X. Li, L. Yu, D. Chang, Z. Ma, and J. Cao, "Dual cross-entropy loss for small-sample fine-grained vehicle classification," *IEEE Transactions on Vehicular Technology*, 2019.

[38] M. Martinez and R. Stiefelhagen, "Taming the cross entropy loss," *arXiv preprint arXiv:1810.05075*, 2018.

[39] K. P. Murphy, *Machine learning: a probabilistic perspective*. MIT press, 2012.

[40] K. Zhang, C. Gao, L. Guo, M. Sun, X. Yuan, T. X. Han, Z. Zhao, and B. Li, "Age group and gender estimation in the wild with deep ror architecture," *IEEE Access*, vol. 5, pp. 22 492–22 503, 2017.

Ke Zhang received the M.E. degree in signal and information processing from North China Electric Power University, Baoding, China, in 2006, and the Ph.D. degree in signal and information processing from the Beijing University of Posts and Telecommunications, Beijing, China, in 2012. He finished his Post Doc in computer vision from the University of Missouri, Columbia, MO, USA, in 2016. He is currently an Associate Professor with North China Electric Power University. His research interests include computer vision, deep learning, machine learning, robot navigation, natural language processing, and spatial relation description.

Xinsheng Wang received the B.S. degree in electronic information science and technology from North China Electric Power University, Baoding, China, in 2017, where he is currently pursuing the master's degree in electronic information science and technology. His research interests include computer vision and deep learning.

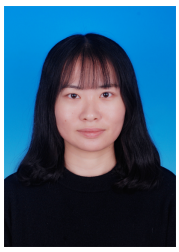

Yurong Guo received the B.S. degree in electronic information science and technology from North China Electric Power University, Baoding, China, in 2017, where she is currently pursuing the master's degree in communication and information engineering. Her research interests include computer vision and deep learning.

Zhenbing Zhao was born in Suqian, Jiangsu, China, in 1979. He received the B.S., M.S., and Ph.D. degrees from North China Electric Power University, Baoding, in 2002, 2005, and 2009, respectively. He is currently an Associate Professor with the School of Electrical and Electronic Engineering, North China Electric Power University. His research interests include machine learning, image processing, and the intelligent detection of electrical equipment.

Zhanyu Ma has been an Assistant Professor with the Beijing University of Posts and Telecommunications (BUPT), Beijing, China, since 2013. He received the M.Eng. degree in signal and information processing from BUPT and the Ph.D. degree in electrical engineering from Royal Institute of Technology (KTH), Stockholm, Sweden, in 2007 and 2011, respectively. From 2012 to 2013, he has been a Post-Doctoral Research Fellow with the School of Electrical Engineering, KTH. His current research interests include statistical modeling and machine learning related topics with a focus on applications in speech processing, image processing, biomedical signal processing, and bioinformatics.

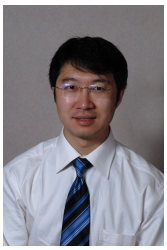

Tony X. Han received the B.S. degree with honors in Electrical Engineering Department and Special Gifted Class from Jiaotong University, Beijing, China in 1998, M.S. degree in electrical and computer engineering from the University of Rhode Island, RI, in 2002, and Ph.D degree in electrical and computer engineering from the University of Illinois at Urbana-Champaign, IL, in 2007. He then joined the Department of Electrical and Computer Engineering at the University of Missouri, Columbia, MO, in August 2007. Currently, he is the CEO of Jingchi.ai. His research interests include machine learning, computer vision, and unmanned vehicle.